Mathematical Sciences
a SpringerOpen Journal

ORIGINAL RESEARCH Open Access

Plane waves reflection in micropolar transversely isotropic generalized thermoelastic half-space

Rajneesh Kumar[1] and Rajani Rani Gupta[2*]

Abstract

Purpose: The purpose of this paper is to study the reflection of plane periodic wave's incident on the surface of generalized thermoelastic micropolar transversely isotropic medium.

Methods: Plane wave propagation is studied to calculate complex velocities of the four waves from the complex roots of a quartic equation. The complex velocity of the attenuated wave in the medium is resolved to calculate its propagation (phase) velocity and quality factor of attenuation. Reflection of waves at the free surface of micropolar transversely isotropic generalized thermoelastic elastic half-space has been discussed.

Results: Numerical examples calculate the amplitude ratios of reflected waves at the free surface of the micropolar transversely isotropic generalized thermoelastic elastic half-space to evince the effects of anisotropy and theories of generalized thermoelasticity.

Conclusions: It is concluded from the present study that there are four quasi wave propagates in of generalized thermoelastic micropolar transversely isotropic medium viz., quasi-longitudinal displacement (qLD) wave, quasi-transverse displacement (qTD) wave, quasi- transverse microrotational (qTM) wave and quasi thermal (qT) waves.

Keywords: Reflection, Micropolar, Transversely isotropic, Amplitude ratio

Background

Depending upon the mechanical properties, the material of the earth has been classified as elastic, viscoelastic, sandy, granular, microstructure, etc. Some parts of the earth may supposed to be composed of material possessing micropolar/granular structure instead of continuous elastic material.

To explain the fundamental departure of microcontinuum theories from the classical continuum theory, the former is a continuum model embedded with microstructures to describe the microscopic motion or a non-local model to describe the long-range material interaction. This extends the application of the continuum model to microscopic space and short-time scale. Micromorphic theory [1,2] treats a material body as a continuous collection of a large number of deformable particles, with each particle possessing finite size and inner structure. Using assumptions such as infinitesimal deformation and slow motion, micromorphic theory can be reduced to Mindlin's microstructure theory (1964). When the microstructure of the material is considered rigid, it becomes the micropolar theory [3].

Eringen's micropolar theory is more appropriate for geological materials like rocks and soil since this theory takes into account the intrinsic rotation and predicts the behavior of material with inner structure. The linear theory of micropolar thermoelasticity was developed by [4] and [5] to include thermal effects and is known as micropolar coupled thermoelasticity.

Inspite of these studies, no attempt has been made to study the reflection of waves in transversely isotropic micropolar generalized thermoelastic medium. Thus, the present study of the effect of anisotropy in a reflection of waves at the free surface of transversely isotropic micropolar generalized thermoelastic medium has its

*Correspondence: rajani_gupta_83@rediffmail.com
[2]Department of Mathematics, National Institute of Technology, Kurukshetra, Haryana, 136 119, India
Full list of author information is available at the end of the article

due importance in engineering and geophysical problems where the situation so demands.

We analyze the reflection of waves in transversely isotropic micropolar generalized thermoelastic medium. This study has many applications in various field of science and technology, namely, atomic physics, industrial engineering, thermal power plants, submarine structures, pressure vessel, aerospace, chemical pipes and metallurgy.

Basic equations

The basic equations in dynamic theory of the plain strain of a homogeneous and micropolar transversely isotropic generalized thermoelastic solid in the absence of body forces, body couples and heat sources are given by the following:

(a) Constitutive relations

$$t_{kl} = A_{klmn}E_{mn} + G_{klmn}\Psi_{mn} - \beta_{kl}(T + \tau_1\dot{T}), \tag{1}$$

$$m_{kl} = B_{lkmn}E_{mn} + G_{mnlk}\Psi_{mn}, \tag{2}$$

$$q_k = K_{kl}T_{,k}, \tag{3}$$

for Lord and Shulman (L-S) theory

$$\rho\eta T_o = \rho C^* T + \beta_{kl}T_o u_{r,r},\ (q_{k,k} + \tau_o\dot{q}_{k,k}) = K_{kl}T_{,kk}, \tag{4}$$

for Green and Lindsay (G-L) theory

$$\rho\eta T_o = \rho C^*(T + \tau_o\dot{T}) + \beta_{kl}T_o u_{r,r},\ q_{k,k} = K_{kl}T_{,kk}. \tag{5}$$

The deformation and wryness tensor are defined by the following:

$$E_{kl} = u_{l,k} + \epsilon_{lkm}\phi_m, \qquad \Psi_{kl} = \phi_{k,l}. \tag{6}$$

(b) Balance laws

$$t_{kl,k} = \rho\ddot{u}_l, \tag{7}$$

$$m_{kl,k} + \epsilon_{lmn}t_{mn} = \rho_J\ddot{\phi}_l, \tag{8}$$

$$q_{k,k} = \rho T_0\dot{\eta}, \tag{9}$$

where t_{kl}, m_{kl}, and K_{kl} are the stress tensor, couple stress tensor and thermal conductivity tensor, respectively; q_k is the heat flux vector; η is the entropy; T is the absolute temperature; C^* is the specific heat at constant strain; τ_0 and τ_1 are the thermal relaxation times; ρ is the bulk mass density; J is the microinertia; u_l and ϕ_k are the components of displacement vector and microrotation vector, respectively; β_{kl} is the thermal elastic coupling tensor; $A_{klmn}, G_{klmn}, B_{lkmn}$ are characteristic constants of material where A_{klmn}, B_{lkmn} satisfies the symmetric properties

$$A_{klmn} = A_{mnkl},\ B_{mnlk} = B_{lkmn}, \tag{10}$$

and $\beta_{kl} = \beta_{lk}$ and $K_{kl} = K_{lk}$. Tensor G_{klmn} does not possess this property; it forms a pseudo-tensor, inversion of the coordinate system changing its sign. In a centrosymmetric body, all components of G_{klmn} vanish.

Formulation of the problem

We have used appropriate transformations following [6] on the set of Equations 1 to 5 to derive equations for micropolar thermoelastic transversely isotopic medium and restricted our analysis to the two-dimensional problem.

We consider a homogeneous, centrosymmetric, micropolar thermoelastic transversely isotropic medium initially in an undeformed state and at uniform temperature T_o. We take the origin of coordinate system on the top plane surface and x_3-axis pointing normally into the half-space, which is thus represented by $x_3 \geq 0$. We consider plane waves such that all particles on a line parallel to x_2-axis are equally displaced, so all partial derivatives with respect to the variable x_2 would be zero. Therefore, we take $\vec{u} = (u_1, 0, u_3)$, $\vec{\phi} = (0, \phi_2, 0)$ and $\partial/\partial x_2 = 0$ so that the field equations and constitutive relations reduce to the following:

$$A_{11}\frac{\partial^2 u_1}{\partial x_1^2} + (A_{13} + A_{56})\frac{\partial^2 u_3}{\partial x_1 x_3} + A_{55}\frac{\partial^2 u_1}{\partial x_3^2} + K_1\frac{\partial \phi_2}{\partial x_3} - \beta_1\left(1 + \tau_1\frac{\partial}{\partial t}\right)\frac{\partial T}{\partial x_1} = \rho\frac{\partial^2 u_1}{\partial t^2}, \tag{11}$$

$$A_{66}\frac{\partial^2 u_3}{\partial x_1^2} + (A_{13} + A_{56})\frac{\partial^2 u_1}{\partial x_1 x_3} + A_{33}\frac{\partial^2 u_3}{\partial x_3^2} + K_2\frac{\partial \phi_2}{\partial x_1} - \beta_3\left(1 + \tau_1\frac{\partial}{\partial t}\right)\frac{\partial T}{\partial x_3} = \rho\frac{\partial^2 u_3}{\partial t^2}, \tag{12}$$

$$B_{77}\frac{\partial^2 \phi_2}{\partial x_1^2} + B_{66}\frac{\partial^2 \phi_2}{\partial x_3^2} - X\phi_2 + K_1\frac{\partial u_1}{\partial x_3} + K_2\frac{\partial u_3}{\partial x_1} = \rho_J\frac{\partial^2 \phi_2}{\partial t^2}, \tag{13}$$

$$K_1^*\frac{\partial^2 T}{\partial x_1^2} + K_3^*\frac{\partial^2 T}{\partial x_3^2} = \rho C^*\left(\frac{\partial}{\partial t} + \tau_o\frac{\partial^2}{\partial t^2}\right)T + T_o\left(\frac{\partial}{\partial t} + n_o\tau_o\frac{\partial^2}{\partial t^2}\right) \times \left(\beta_1\frac{\partial u_1}{\partial x_1} + \beta_3\frac{\partial u_2}{\partial x_2}\right). \tag{14}$$

$$t_{33} = A_{13}\frac{\partial u_1}{\partial x_1} + A_{33}\frac{\partial u_3}{\partial x_3} - \beta_3(1+\tau_1\frac{\partial}{\partial t})T, \tag{15}$$

$$t_{31} = A_{65}\frac{\partial u_3}{\partial x_1} + K_1\phi_2 + A_{55}\frac{\partial u_1}{\partial x_3}, \tag{16}$$

$$m_{32} = B_{66}\frac{\partial \phi_2}{\partial x_3}, \tag{17}$$

where $\beta_1 = A_{11}\alpha_1 + A_{13}\alpha_3$, $\beta_3 = A_{31}\alpha_1 + A_{33}\alpha_3$, $K_1 = A_{56} - A_{55}$, $K_2 = A_{66} - A_{56}$, $X = K_2 - K_1$, α_1, α_3 are the coefficients of linear thermal expansion, we have used the notations $11 \to 1$, $33 \to 3$, $12 \to 7$, $13 \to 6$, $23 \to 5$ for the material constants.

For L-S theory $\tau_1 = 0$, $n_o = 1$; for G-L theory, $\tau_1 > 0$, $n_o = 0$; and for coupled thermoelasticity theory, $n_o = 0, \tau_1 = \tau_o = 0$. The thermal relaxation times τ_0 and τ_1 satisfy the inequality $\tau_1 \geq \tau_0 > 0$ for G-L theory only. However, it has been proved by [7] that the inequalities are not mandatory for τ_0 and τ_1 to follow.

For further considerations, it is convenient to introduce the dimensionless variables defined by the following:

$$\begin{aligned}
&x_1' = \frac{\omega^*}{c_1}x_1,\ x_3' = \frac{\omega^*}{c_1}x_3,\ u_1' = \frac{\omega^*}{c_1}u_1,\ u_3' = \frac{\omega^*}{c_1}u_3,\\
&\phi_2' = \frac{A_{55}}{K_1}\phi_2,\ t_{ij}' = \frac{t_{ij}}{A_{11}},\\
&m_{ij}' = \frac{m_{ij}c_1}{B_{56}\omega^*},\ T' = \frac{T}{T_o},\ t' = \omega^* t,\ \tau_o' = \omega^*\tau_o,\\
&\tau_1' = \omega^*\tau_1,\ \omega^{*2} = \frac{X}{\rho_J},\ c_1^2 = \frac{A_{11}}{\rho},
\end{aligned} \tag{18}$$

where ω^* is the characteristic frequency of the material, and c_1 is the longitudinal wave velocity of the medium.

Plane-wave propagation

Let $\overrightarrow{p}(p_1, 0, p_3)$ denotes the unit propagation vector, c and k are the phase velocity and the wave number of the plane waves propagating in x_1x_3 plane, respectively. We seek plane-wave solution of the equations of motion of the form

$$(u_1, u_3, \phi_2, T) = (\bar{u}_1, \bar{u}_3, \bar{\phi}_2, \bar{T})e^{\iota\xi(p_1x_1 + p_3x_3 - ct)}. \tag{19}$$

Making use of Equation 18 and the values of u_1, u_3, ϕ_2 and T from Equation 19 in the Equations 11 to 14, we obtain four homogeneous equations in four unknowns $\bar{u}_1, \bar{u}_3, \bar{\phi}_2$ and $\bar{T}$, which for the non-trivial solution yield

$$Ac^8 + Bc^6 + Cc^4 + Dc^2 + E = 0, \tag{20}$$

where

$$\begin{aligned}
&A = b_4 - b_5/\omega^2,\ B = g_1 + g_6/\omega^2,\\
&C = g_3 + (g_2 + g_4)/\omega^2 + g_4/\omega^4,\ D = g_5 + g_7/\omega^2,\\
&E = g_8,\ g_1 = b_1 - b_2' - b_4a_1,\ g_2 = b_8 - b_2 - b_4a_1\\
&\quad + b_{17}a_{14} + b_{12}a_{15} - a_1b_5, g_3 = b_6' - b_1 - b_3\\
&\quad + b_2'a_1 + b_{12}'a_{10},\ g_4 = b_6 + a_1b_2 + a_{10}\\
&\quad \times (b_{12} - b_{13}') + a_{14}(b_{15} - b_{18} + b_{15}') - a_{15}b_{18},\\
&g_5 = b_7 + b_3a_1 + b_9a_{10} - a_1b_6',\ g_6 = b_5a_1 - a_{15}b_{22},\\
&g_7 = b_{14}a_{14} + b_{20}a_{15} - b_6a_1 - a_{10}b_{10},\ g_8 = -b_7a_1\\
&\quad - b_{11}a_{10},\ g_9 = b_{19}a_{15} - a_1b_8 - a_{10}b_{13},\\
&b_1 = d_7a_8d_{12},\ d_1 = \frac{A_{55}}{A_{11}},\ d_2 = \frac{(A_{13} + A_{56})}{A_{11}},\\
&d_3 = \frac{K_1^2}{A_{11}A_{55}},\ d_4 = \frac{A_{66}}{A_{11}},\ d_5 = \frac{A_{33}}{A_{11}},\ d_6 = \frac{K_1K_2}{A_{11}A_{55}},\\
&d_7 = \frac{B_{66}}{\rho_J c_1^2},\ d_8 = \frac{B_{77}}{\rho_J c_1^2},\ d_9 = \frac{X}{\rho_J\omega^{*2}},\ d_{10} = \frac{A_{55}}{\rho_J\omega^{*2}},\\
&d_{11} = \frac{K_2}{K_1}d_{10},\ d_{13} = \frac{\beta_3T_o}{A_{11}},\ d_{18} = \frac{A_{13}}{A_{11}},\ d_{14} = \frac{\beta_1T_o}{A_{11}},\\
&d_{15} = \frac{K_1^*}{A_{55}},\ ,\ d_{16} = \frac{A_{56}}{A_{11}}\bar{\beta} = \frac{\beta_1}{\beta_3},\ \bar{K} = \frac{K_1^*}{K_3^*},\\
&\varepsilon_1 = \frac{\rho C^*c_1^2}{K_3^*\omega^*},\ \varepsilon_2 = \frac{\beta_3c_1^2}{K_3^*\omega^*}.b_2 = d_7(a_8d_{11} + d_9d_6)\\
&\quad + a_7a_4d_{12},\ b_2' = a_2a_9d_{12},\ b_3 = a_8(a_6d_7 + a_2d_{12}),\\
&b_4 = d_{12}d_7a_9,\ b_5 = d_7d_{11}a_9,\ b_6 = a_6a_7a_4\\
&\quad + a_8(a_2d_{11} - a_3a_5),\ b_6' = a_2a_6a_9,\\
&b_8 = a_9(a_2d_{11} - a_3a_5), b_7 = a_2a_6a_8,\ b_9 = a_8a_{11}d_{12},\\
&b_{10} = a_{11}(a_8d_{11} + a_6d_9) + a_5a_8a_{12} - a_6a_7a_{13},\\
&b_{11} = a_8a_6a_{11},\ b_{12} = -a_7a_{13}d_{12},\ b_{12}' = a_9a_{11}d_{12},\\
&b_{13} = a_7a_{13}d_{11},\ b_{13}' = a_9(a_{11}d_{12} + a_5a_{12}),\\
&b_{14} = a_8(a_1a_3 + a_2a_{12}),\ b_{15} = a_7(a_4a_{12} - a_3a_{13}),\\
&b_{15}' = a_9(a_1a_3 + a_2a_{12}),\ b_{16} = a_8a_{12}d_7,\\
&b_{17} = -a_9a_{12}d_7,\ b_{18} = d_{12}(a_4a_{11} + a_2a_{13}),\\
&b_{19} = d_{11}(a_{14}a_4 + a_2a_{13}) - a_6a_{13}d_7\\
&\quad + a_5(a_4a_{11} - a_3a_{13}),\ b_{20} = a_6(a_4a_{11} + a_2a_{13}),\\
&b_{21} = a_{13}d_{12}d_7,\ b_{22} = a_{13}d_7d_{11},\ a_1 = d_1p_3^2 + p_1^2,\\
&a_2 = d_5p_3^2 + p_1^2d_4,\ a_3 = \iota p_1d_{10},\ a_4 = p_3\omega\varepsilon_2(1 - \iota\omega\tau_1),
\end{aligned}$$

$$a_5 = \iota p_1 d_6,\ a_6 = d_7 p_3^2 + p_1^2 d_8,\ a_7 = -\iota p_3 d_{14} \times (1 - \iota\omega\tau_1),\ a_8 = p_3^2 + \bar{k} p_1^2,\ a_9 = -\iota\varepsilon_1 \times (1/\omega - \iota\tau_o),\ a_{10} = p_1 p_3 d_2,\ a_{11} = -p_1 p_3 d_5,$$
$$a_{12} = \iota p_3 d_9,\ a_{13} = p_3\omega\varepsilon_2 p_1\bar{\beta}(1 - \iota\omega\tau_1),\ a_{14} = \iota p_3 d_3,$$
$$a_{15} = -\iota p_1 d_3(1 - \iota\omega\tau_1). \quad (21)$$

The complex coefficient implies that four roots of this equation may be complex. The complex phase velocities of the quasi-waves, given by $c_i, i = 1,2,3,4$, will be varying with the direction of phase propagation. The complex velocity of a quasi-wave, i.e. $c_i = c_R + \iota c_I$, defines the phase propagation velocity $V_i = (c_R^2 + c_I^2)/c_R$ and attenuation quality factor $Q_i^{-1} = -2c_I/c_R$ for the corresponding wave. Therefore, four waves propagating in such a medium are attenuating. The same directions of wave propagation and attenuation vector of these waves make them homogeneous wave. These waves are called quasi-waves because polarizations may not be along the dynamic axes. The waves with velocity $V_i (i = 1,2,3,4)$ may be named as quasi-longitudinal displacement (qLD) wave, quasi-transverse displacement (qTD) wave, quasi-transverse microrotational (qTM) wave and quasi thermal wave (qT) that are propagating with the descending phase velocities, respectively.

Reflection at the free surface

We consider a homogeneous micropolar generalized thermoelastic transversely isotropic half-space occupying the region $x_3 > 0$. Incident qLD or qTD or qTM or qT wave at the interface will generate reflected qLD, qTD, qTM and qT waves in the half-space $x_3 > 0$. The total displacements, microrotation and temperature distribution are given by the following:

$$u_1 = \sum_{j=1}^{8} A_j e^{\iota E_j},\ u_3 = \sum_{j=1}^{8} B_j e^{\iota E_j},$$
$$\phi_2 = \sum_{j=1}^{8} C_j e^{\iota E_j},\ T = \sum_{j=1}^{8} D_j e^{\iota E_j}, \quad (22)$$

where

$$E_j = \omega[\, t - (x_1 sine_j - x_3 cose_j)/c_j\,],\ j = 1,2,3,4, \quad (23)$$

$$E_j = \omega[\, t - (x_1 sine_j + x_3 cose_j)/c_j\,],\ j = 5,6,7,8, \quad (24)$$

ω is the angular frequency. Here, subscripts 1,2,3, and 4 denote the quantities corresponding to incident qLD, qTD, qTM and qT wave, respectively, whereas the subscripts 5,6,7 and 8, respectively, denote the corresponding reflected waves and

$$B_j = \frac{\Lambda_{1i}}{\Lambda_i} A_j,\ C_j = \frac{\Lambda_{2i}}{\Lambda_i} A_j,\ D_j = \frac{\Lambda_{3i}}{\Lambda_i} A_j,\ (j = 1,\ldots,8),$$

$$\Lambda_i = \begin{vmatrix} d_7\omega^2 - \xi^2 a_2 & \xi a_5 & \xi a_7 \\ \xi a_3 & \omega^2 - d_{11} - \xi^2 a_6 & 0 \\ \xi a_4 & 0 & a_9 + a_8\xi^2 \end{vmatrix},$$

$$\Lambda_{1i} = \begin{vmatrix} \xi^2 a_{11} & \xi a_5 & \xi a_7 \\ \xi a_{12} & \omega^2 - d_{11} - \xi^2 a_6 & 0 \\ \xi a_{13} & 0 & a_9 + a_8\xi^2 \end{vmatrix},$$

$$\Lambda_{2i} = \begin{vmatrix} \xi^2 a_{11} & d_7\omega^2 - \xi^2 a_2 & \xi a_7 \\ \xi a_{12} & \xi a_3 & 0 \\ \xi a_{13} & \xi a_4 & a_9 + a_8\xi^2 \end{vmatrix},$$

$$\Lambda_{3i} = \begin{vmatrix} \xi^2 a_{11} & d_7\omega^2 - \xi^2 a_2 & \xi a_5 \\ \xi a_{12} & \xi a_3 & \omega^2 - d_{11} - \xi^2 a_6 \\ \xi a_{13} & \xi a_4 & 0 \end{vmatrix}. \quad (25)$$

The expressions for a_i, $i = 1,2,....15$ are obtained from the expressions for a_i, $i = 1,2,....15$ given in Equation 21 on substituting the values for p_1 and p_2.

For incident qLD wave, $p_1 = sine_1, p_3 = -cose_1$; for incident qTD wave, $p_1 = sine_2, p_3 = -cose_2$; for incident qTM wave, $p_1 = sine_3, p_3 = -cose_3$; for incident qT wave, $p_1 = sine_4, p_3 = -cose_4$; for reflected qLD wave, $p_1 = sine_5, p_3 = cose_5$; for reflected qTD wave, $p_1 = sine_6, p_3 = cose_6$; for reflected qTM wave, $p_1 = sine_7, p_3 = cose_7$; and for reflected qT wave, $p_1 = sine_8, p_3 = cose_8$.

Boundary condition

We assume that the boundaries of the half-space are stress-free thermally insulated. Therefore, the appropriate boundary conditions at the surface $x_3 = 0$ are as follows:
(a) Vanishing of the normal stress

$$t_{33} = 0, \quad (26)$$

(b) Vanishing of the tangential stress

$$t_{31} = 0, \quad (27)$$

(c) Vanishing of the tangential couple stress

$$m_{32} = 0, \quad (28)$$

(d) Vanishing of the temperature gradient

$$\frac{\partial T}{\partial y} + hT = 0 = 0, \quad (29)$$

where h is the surface heat transfer coefficient;
$h \longrightarrow 0$ corresponds to thermally insulated boundaries and $h \longrightarrow \infty$ refers to isothermal boundaries.

The boundary conditions given by Equations 27 to 30 must be satisfied for all values of x_1 and t, so we have

$$E_1(x_1, 0, t) = E_2(x_1, 0, t) = ... = E_8(x_1, 0, t). \tag{30}$$

Then from Equations 23, 24 and 31, we have

$$\frac{sine_1}{c_1} = \frac{\sin e_2}{c_2} = ... = \frac{\sin e_7}{c_7} = \frac{\sin e_8}{c_8} = \frac{1}{c}, \tag{31}$$

which corresponds to the Snell's law in the present case and

$$\xi_1 c_1 = \xi_2 c_2 = ... = \xi_8 c_8 = \omega. \tag{32}$$

Here, $e_1 = e_5$, $e_2 = e_6$, $e_3 = e_7$ and $e_4 = e_8$ i.e. the angle of incidence is equal to the angle of reflection in micropolar transversely isotropic generalized thermoelastic solid so that the velocities of reflected waves are equal to their corresponding incident waves, i.e. $c_1 = c_5$, $c_2 = c_6$, $c_3 = c_7$ and $c_4 = c_8$.

Making use of Equations 15 to 18, 22, 31 and 32 in the boundary conditions given by Equations 26 to 29, we obtain four simultaneous equations as follows:

$$\sum_{j=1}^{8} A_{ij} A_j = 0, \ (i = 1, ..., 4), \tag{33}$$

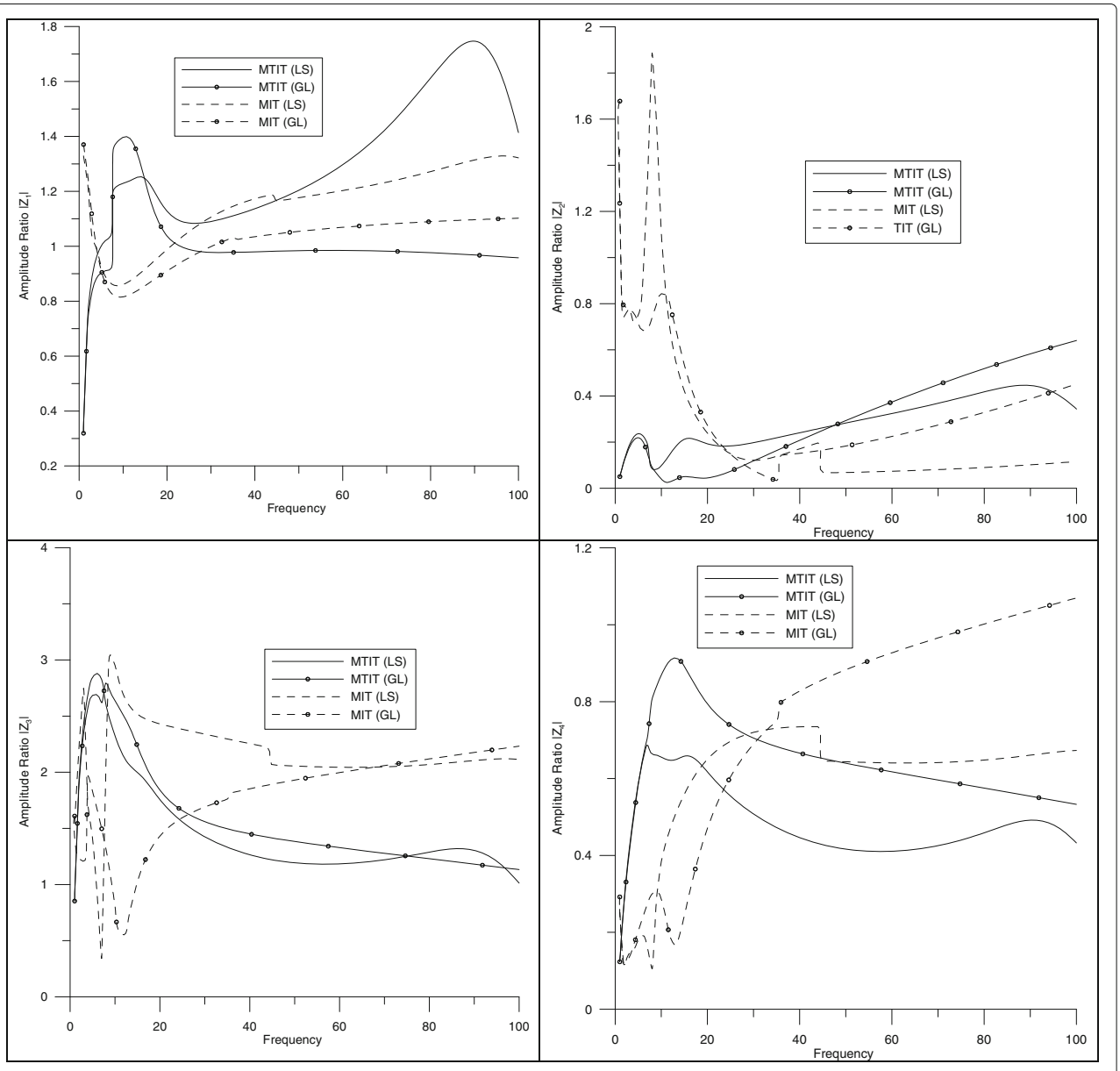

Figure 1 a) $|Z_1|$ b) $|Z_2|$ c) $|Z_3|$ d) $|Z_4|$ for incident qLD wave.

where

$$A_{1j} = -d_{18}\frac{\sin e_j}{c_j} + r_j d_5 \frac{\cos e_j}{c_j} - t_j d_{13}(1+\tau_1\omega),\ j = 1,..4,$$

$$A_{1j} = -d_{18}\frac{\sin e_j}{c_j} - r_j d_5 \frac{\cos e_j}{c_j} - t_j d_{13}(1+\tau_1\omega),\ j = 5,..8,$$

$$A_{2j} = d_1\frac{\cos e_j}{c_j} - d_{16} r_j \frac{\sin e_j}{c_j} + d_{17} s_j,\ j = 1,..4,$$

$$A_{2j} = -d_1\frac{\cos e_j}{c_j} - d_{16} r_j \frac{\sin e_j}{c_j} + d_{17} s_j,\ j = 5,..8$$

$$A_{3j} = d_{15} s_j \frac{\cos e_j}{c_j},\ A_{4j} = t_j \frac{\cos e_j}{c_j},\ j = 1,..4,$$

$$A_{3j} = -d_{15} s_j \frac{\cos e_j}{c_j},\ A_{4j} = -t_j \frac{\cos e_j}{c_j},\ j = 5,..8.$$

In case of incident qLD wave, $A_2 = A_3 = A_4 = 0$. Dividing set of Equation 33 throughout by A_1, we obtain a system of four non-homogeneous equations in four unknowns which can be solved by Gauss elimination method and we have

$$Z_i = \frac{A_{i+4}}{A_1} = \frac{\triangle_i^1}{\triangle}(i = 1, ..., 4) \tag{34}$$

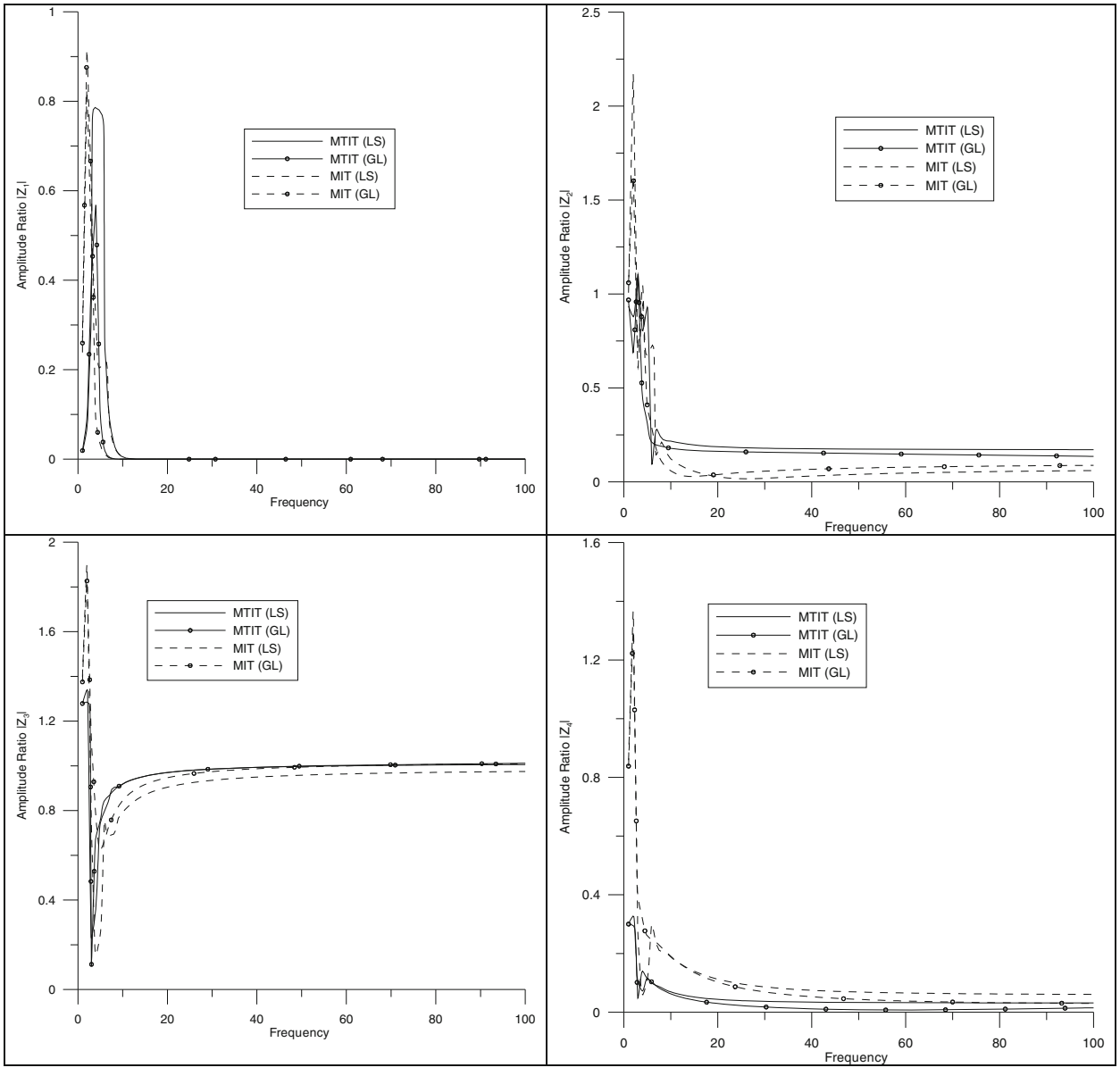

Figure 2 a) $|Z_1|$ b) $|Z_2|$ c) $|Z_3|$ d) $|Z_4|$ for incident qTD wave.

In case of incident qTD wave, $A_1 = A_3 = A_4 = 0$ and thus we have

$$Z_i = \frac{A_{i+4}}{A_2} = \frac{\triangle_i^2}{\triangle}(i = 1, ..., 4) \tag{35}$$

In case of incident qTM wave, $A_1 = A_2 = A_4 = 0$ and thus we have

$$Z_i = \frac{A_{i+4}}{A_3} = \frac{\triangle_i^3}{\triangle}(i = 1, ..., 4) \tag{36}$$

In case of incident qT wave, $A_1 = A_2 = A_3 = 0$ and thus we have

$$Z_i = \frac{A_{i+4}}{A_1} = \frac{\triangle_i^4}{\triangle}(i = 1, ..., 4) \tag{37}$$

where

$$\triangle = |A_{ii+4}|_{4\times 4},$$

and $\triangle_i^p (i = 1, 2, .., 4)(p = 1, ..., 4)$ can be obtained by replacing, respectively, the 1st, 2nd,..., 4th columns of $\triangle$ by $[-A_{1p}, -A_{2p}, -A_{3p}, -A_{4p}]^T$.

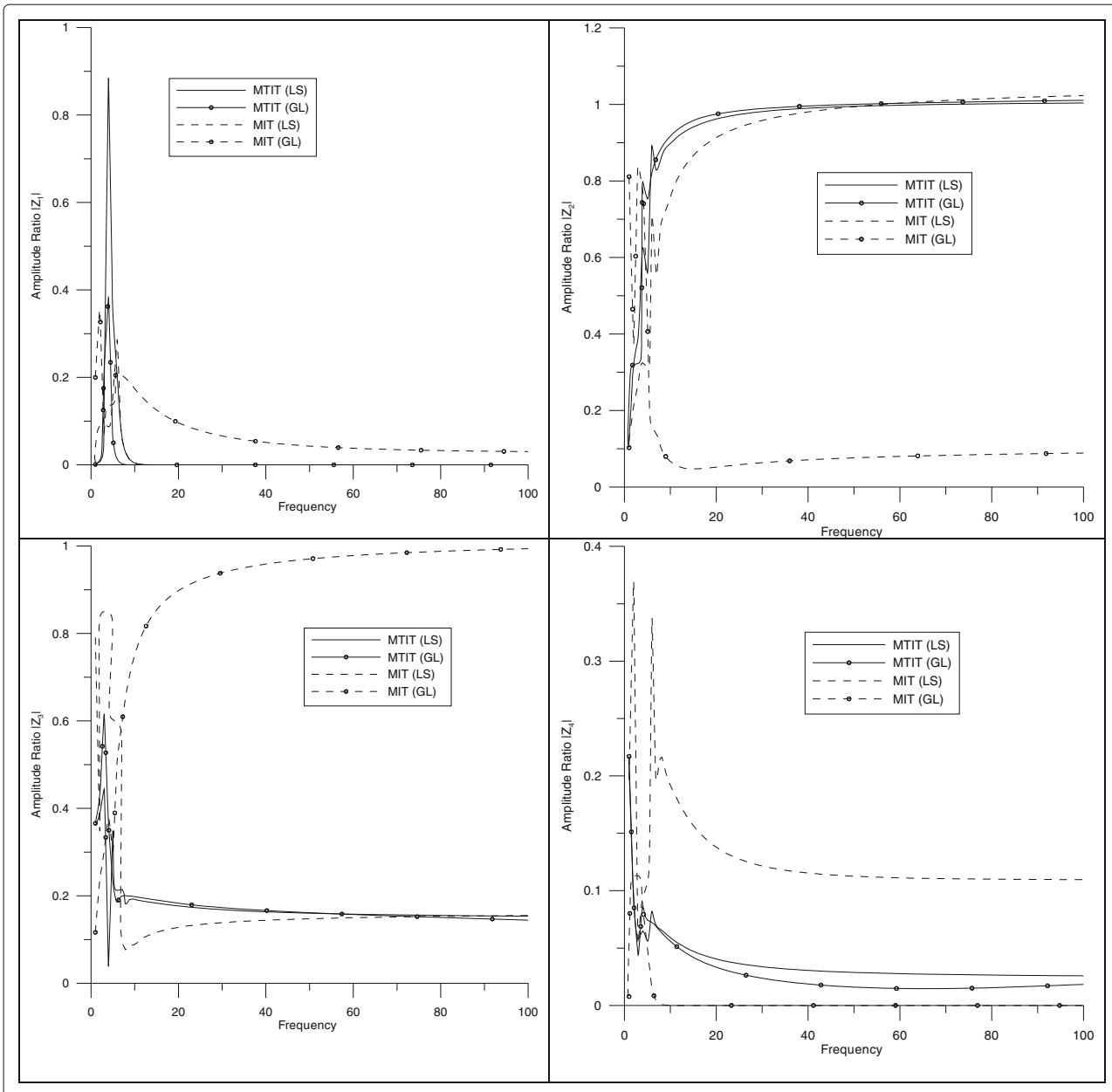

Figure 3 a) $|Z_1|$ b) $|Z_2|$ c) $|Z_3|$ d) $|Z_4|$ for incident qTM wave.

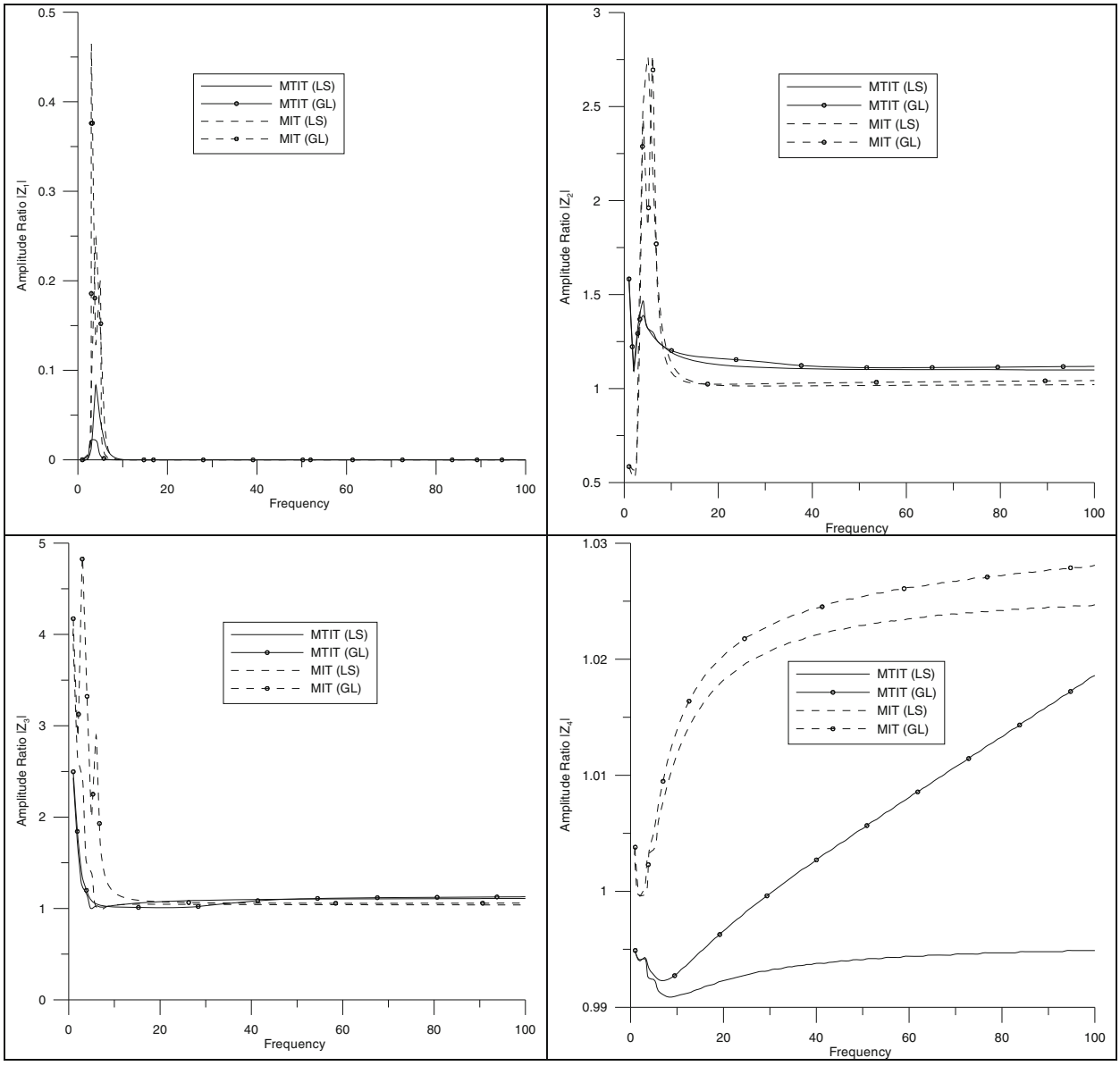

Figure 4 a) $|Z_1|$ b) $|Z_2|$ c) $|Z_3|$ d) $|Z_4|$ for incident qT wave.

Numerical results and discussion

In order to illustrate the theoretical results obtained in the preceding sections, we now present some numerical results. For numerical computation, we take the values for relevant parameters for micropolar transversely isotropic generalized thermoelastic medium as follows:

$$A_{11} = 21.4 \times 10^9 N/m^2,\ A_{77} = 5.4 \times 10^9 N/m^2,$$
$$A_{88} = 5.2 \times 10^9 N/m^2,\ A_{22} = 20.24 \times 10^9 N/m^2,$$
$$A_{12} = 9.4 \times 10^9 N/m^2,\ A_{78} = 4.0 \times 10^9 N/m^2,$$
$$B_{44} = .779 \times 10^5 N,\ B_{66} = .779 \times 10^5 N.$$

Following [8], we take the non-dimensional values for aluminium epoxy-like composite as follows:

$$\rho = 2.19 \times 10^3 kg/m^3,\ \lambda = 9.4 \times 10^9 N/m^2,$$
$$\mu = 4.0 \times 10^9 N/m^2,\ K = 1. \times 10^9 N/m^2,$$
$$C^* = 1.04 Cal/K,\ \gamma = 0.779 \times 10^5 N,\ \jmath = 0.2 \times 10^{-4} m^2.$$

Figures 1,2,3,4 give the graphical representation for the variations of amplitude ratios of reflected qLD, qTD, qTM and qT waves when four types of waves *viz.* qLD, qTD, qTM and qT are incident at the free surface to compare

the results in two cases, (a) the waves incident from MTIT and (b) the waves incident from MIT medium. Figure 1 represents graphically the variations of amplitude ratios $|Z_1|, |Z_2|, |Z_3|$ and $|Z_4|$ in case of incident qLD wave. Figures 2,3,4 show similar cases for incident qTD, qTM and qT waves, respectively. Here, $|Z_1|, |Z_2|, |Z_3|$ and $|Z_4|$ are the amplitude ratios of reflected qLD, qTD, qTM and qT waves, respectively. These variations are shown for two theories of thermoelasticity, *viz.* L-S and G-L. In these figures, the solid and broken curves without center symbol correspond to the case of L-S theory, while solid and broken curves with center symbol ($-\circ-\circ-$) correspond to the case of G-L theory.

Incident qLD wave

It is evident from Figure 1a that the amplitude ratio $|Z_1|$ of reflected qLD wave first increases sharply, then oscillates within the interval $7 < \omega < 15$ and decreases with further increase in frequency for MTIT. However, for MIT, its value initially oscillates and then increases a little to become a constant at the end with increase in frequency. This behavior is noticed for both cases of L-S and G-L theories.

Figure 1b,c indicates the variations of amplitude ratios $|Z_2|$ and $|Z_3|$ of reflected qTD and qTM waves, which show that for the case of G-L theory and MTIT, their value increases with increase in frequency, while in the case of L-S theory, its value starts varying with initial increase then becomes constant for some time and then increases again with increase in frequency. Similar variations are noticed for MIT, except for G-L theory, where its value tends to decrease at the end. It is depicted from Figure 1d that the value of amplitude ratio $|Z_4|$ goes on increasing with increase in frequency in all the cases.

Incident qTD wave

The variations in the amplitude ratio of various reflected wave for incident qTD wave are shown in Figure 2. It is depicted from Figure 2a that the value of amplitude ratio of $|Z_1|$ sharply increases to a peak value and oscillate to become constant. Similar variations are noticed for the case of G-L theory with slight difference in their amplitude. However, for MIT, its value initially oscillates with varying amplitude and then flattens to become zero at the end for both cases of L-S and G-L theories.

It can be seen from Figure 2b that for L-S theory, the value of amplitude ratio $|Z_2|$ for MTIT initially oscillates with a hump in the interval $10 \leq \omega \leq 40$ and then decreases. While for G-L theory, its value initially oscillates and then decreases to attain a constant value with increase in frequency. For MIT and for both theories of thermoelasticity, their values start with initial oscillation to become constant. It is evident from this figure that the the amplitude ratio gets increased due to anisotropy.

Figure 2c,d shows the variations of amplitude ratio $|Z_3|$ and $|Z_4|$ within the interval $0 \leq \omega \leq 30$, oscillate arbitrarily with different amplitude and then become constant with increase in frequency. The similar variations are depicted for all the curves, except for MIT and G-L theory where the value of amplitude ratio $|Z_3|$ decreases with increase in frequency, while the value of amplitude ratio $|Z_4|$ increases with increase in frequency.

Incident qTM wave

Figure 3 illustrates the variations of amplitude ratios of $|Z_i|, i = 1, 2, 3, 4$, with frequency for incident qTM wave. It can be seen from these figures that the variation pattern of the amplitudes are almost similar with difference in their peak values. Their values show a hump within an interval and after that they tend to attain a constant value. The amplitude ratio of the first two waves gets increased due to anisotropy, while for the remaining, their values show oscillatory nature. The amplitude ratios $|Z_1|$ and $|Z_2|$ have higher values for L-S theory as compared to those for G-L theory, while the remaining amplitudes, initially the values are higher for L-S theory and reverse behavior is noticed afterwards.

Incident qT wave

The variations in amplitude ratio of various reflected waves for incident qT wave are shown in Figure 4. The amplitude ratio $|Z_1|$ sharply decreases to become constant for MIT, while for the case of MTIT, its value sharply increases then sharply decrease to become constant at the end. Slight differences in their amplitudes have been observed. The variations of $|Z_2|$ and $|Z_3|$ are shown in Figure 4b,c. It can be seen from these figures that the values oscillate within the interval $0 \leq \omega \leq 30$, showing the peaks of different amplitudes. After this interval, the values for all the cases become steady.

Figure 4d shows the variations in the value of $|Z_4|$, which indicates that anisotropy as well as angle of incidence shows a significant impact on it throughout the whole range. The behavior of $|Z_4|$ is oscillatory within the range $0 \leq \omega \leq 30$. The amplitude ratio $|Z_4|$ first increases from small value to a maximum by executing small oscillation and ultimately decreases to become steady. The value for the case of L-S theory is higher as compared to those for G-L theory. Anisotropy shows a greater impact on $|Z_4|$ as compared to the relaxation times.

Conclusion

Propagation of waves in a micropolar transversely isotropic generalized thermoelastic half-space have been discussed. The amplitude ratios have been computed and plotted graphically for L-S and G-L theories of

thermoelasticity. It is concluded from the figures that the value of amplitude ratios $|Z_1|, |Z_2|$ and $|Z_3|$ shows sharp oscillation at initial frequencies for incident qLD and qT waves as compared to qTM and qTD incident waves. An appreciable effects of anisotropy and relaxation time are noticed on amplitude ratios of various reflected waves.

Competing interests
The authors declare that they have no competing interests.

Author's contributions
RK formulated the problem. RRG drafted the manuscript and aligned the manuscript sequentially. She also carried out the numerical computations and interpret them graphically. Both authors read and approved the final manuscript.

Author details
[1]Department of Mathematics, Kurukshetra University, Kurukshetra, Haryana, 136 119, India. [2]Department of Mathematics, National Institute of Technology, Kurukshetra, Haryana, 136 119, India.

Received: 23 February 2010 Accepted: 29 May 2012
Published: 29 May 2012

References

1. Suhubi, ES, Eringen, AC: Non-linear theory of simple microelastic solids II. International Journal of Engineering Science. **2**, 389–404 (1964)
2. Eringen, AC: Microcontinuum Field Theories I: Foundations and Solids. Springer-Verlag, New York (1999)
3. Eringen, AC: Linear theory of micropolar elasticity. Journal of Mathematical Mechanics. **16**, 909–923 (1966)
4. Eringen, AC: Foundations of Micropolar Thermoelasticity. Course of Lectures No.23 . CSIM Udine Springer, Berlin (1970)
5. Nowacki, M: Couple-stresses in the theory of thermoelasticity . In *Proc. IUTAM Symposia, Vienna,* June 22-28 1996. Edited by: Parkus, H, Sedov, LI. Springer-Verlag, New York, 259-278 (1996)
6. Slaughter, WS: The Linearized Theory of Elasticity . Birkhauser, Basel (2002)
7. Strunin, DV: On characteristic times in generalized thermoelasticity. Journal of Applied Mechanics. **68**, 816–817 (2001)
8. Gauthier, RD: In experimental investigations on micropolar media . In *Mechanics of Micropolar media*. Edited by: Brulin, O, Hsieh, RKT. World Scientific, Singapore (1982)

doi:10.1186/2251-7456-6-6
Cite this article as: Kumar and Gupta: **Plane waves reflection in micropolar transversely isotropic generalized thermoelastic half-space.** *Mathematical Sciences* 2012 **6**:6.